Sublattice extraordinary-log phase and special points of the antiferromagnetic Potts model

Li-Ru Zhang,[1] Chengxiang Ding,[1,*] Wanzhou Zhang,[2] and Long Zhang[3,†]

[1]*School of Microelectronics & Data Science, Anhui University of Technology, Maanshan, Anhui 243002, China*

[2]*College of Physics and Optoelectronics, Taiyuan University of Technology, Taiyuan, Shanxi 030024, China*

[3]*Kavli Institute for Theoretical Sciences and CAS Center for Excellence in Topological Quantum Computation, University of Chinese Academy of Sciences, Beijing 100190, China*

(Received 26 January 2023; revised 22 June 2023; accepted 22 June 2023; published 5 July 2023)

We study the surface criticality of a three-state antiferromagnetic Potts model on a simple cubic lattice, whose bulk critical behavior belongs to the universality class of the XY model because of emergent O(2) symmetry. We find that the surface antiferromagnetic next-nearest-neighboring interactions can drive the extraordinary-log phase to an ordinary phase, and the transition between the two phases belongs to the universality class of the well-known special transition of the XY model. Further enhancing the surface next-nearest-neighboring interactions, the extraordinary-log phase reappears, but the main critical behaviors are shown in the sublattices; the special point between the ordinary phase and the sublattice extraordinary-log phase belongs to a different universality class.

DOI: 10.1103/PhysRevB.108.024402

I. INTRODUCTION

For a system at the critical point of a continuous phase transition, the correlation function and order parameter and some other physical quantities exhibit power-law scaling behaviors, which are called critical behaviors. At a critical point, the critical behaviors not only manifest in the bulk but also on the surface, which are called surface critical behaviors [1,2]. Depending on the strength of the surface interactions, the surface critical behaviors can be richer than the bulk critical behaviors. Generally, there are three types of surface critical phases, dubbed "ordinary phase," "special point," and "extraordinary phase." An ordinary phase refers to the case when the surface interactions are not too strong, and the surface critical behaviors are purely induced by the bulk critical state; the extraordinary phase refers to the case when the surface interactions are strong enough, and the surface has become ordered or critical with logarithmic scaling behaviors (extraordinary-log phase); the special point is the transition point between the ordinary phase and the extraordinary phase. Typical examples can be found in classical O(n) spin models [3–6].

The research on surface critical behaviors has a long history, and the interest in this field is renewed by recent works on quantum spin models [7,8]. A series of related studies has greatly promoted the research in this field [9–23], which includes the prediction of an extraordinary-log phase [11], a different type of surface criticality. In such a phase, the surface two-point correlation function $G_{\parallel}(r)$ decays logarithmically with r as

$$G_{\parallel}(r) \propto [\ln(r/r_0)]^{-q}, \tag{1}$$

where q is a universal decaying exponent and r_0 is a nonuniversal parameter; this is very different from the power-law decaying correlation function of a traditional critical point. The extraordinary-log phase has already been numerically found in both classical spin models [5,6,20] and also quantum spin models [22,23].

In our recent work [20], we found an extraordinary-log phase in the three-state antiferromagnetic Potts model on a simple cubic lattice, which has a bulk critical point belonging to the universality class of the XY model because of the emergent O(2) symmetry [24], although the spin symmetry of the model is discrete. Tuning the surface nearest-neighboring (NN) interactions leads to a surface phase diagram similar to that of the XY model. More importantly, by adding *ferromagnetic* next-nearest-neighboring (NNN) interactions to the surface, a phase transition from the extraordinary-log phase to a symmetry-breaking phase is found, whose critical behaviors are very different from the traditional ordered-disordered phase transition. That such a type of phase transition can be realized is related to the bulk critical point with emergent O(2) symmetry and that a two-dimensional (2D) (square-lattice) three-state Potts model with antiferromagnetic NN interactions and ferromagnetic NNN interactions can be ordered in the low-temperature region [25].

However, according to our understanding, if both NN and NNN interactions are antiferromagnetic, the 2D square-lattice three-state Potts model cannot be ordered even when the temperature is zero [26]; the interplay between such 2D physics and 3D bulk criticality may lead to interesting surface criticality. Therefore, in the current paper, we add *antiferromagnetic* NNN interactions to the surface of the three-state antiferromagnetic Potts model on a simple cubic lattice, and we find that the antiferromagnetic NNN interactions can drive the surface from the extraordinary-log phase to an ordinary phase, then driving the system to an extraordinary-log phase

*dingcx@ahut.edu.cn

†longzhang@ucas.ac.cn

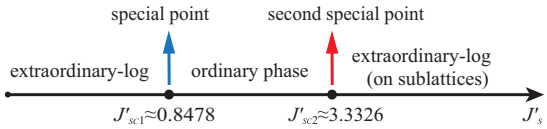

FIG. 1. Surface phase diagram of the antiferromagnetic Potts model (2) with $T = T_c^{\text{bulk}} = 1.226\,03$ and $J_s = 5$.

whose main critical behaviors are shown in the sublattices if the strengths of the NNN interactions are strong enough. The universality class of the special point between the ordinary phase and the sublattice extraordinary-log phase is different from the well-known special point of the XY model.

The paper is organized as follows: In Sec. II, we introduce the model and the method; in Sec. III, we present the numerical results, which include the critical properties of the two special points, the ordinary phase and the sublattice extraordinary-log phase. We conclude our paper in Sec. IV.

II. MODEL AND METHOD

The Hamiltonian of the three-state antiferromagnetic Potts model with surface NNN interactions on a simple cubic lattice is defined as

$$\mathcal{H} = J\sum_{\langle i,j\rangle}\delta_{\sigma_i,\sigma_j} + J_s\sum_{\langle i,j\rangle^s}\delta_{\sigma_i,\sigma_j} + J'_s\sum_{\langle\langle i,j\rangle\rangle'}\delta_{\sigma_i,\sigma_j}, \tag{2}$$

where $\langle i,j\rangle$, $\langle i,j\rangle^s$, and $\langle\langle i,j\rangle\rangle'$ denote the bulk NN, the surface NN, and the surface NNN sites, respectively. All the interactions are antiferromagnetic, and the strength of the bulk interactions is set to be $J = 1$. The spin σ_i can be mapped to a unit vector on the plane,

$$\vec{\sigma}_i = (\cos\theta_i, \sin\theta_i), \tag{3}$$

with $\theta_i = 2\pi\sigma_i/3$ and $\sigma_i = 1, 2, 3$. The bulk phase transition of the model belongs to the XY universality class because of emergent O(2) symmetry [24], and the critical point has been refined by extensive Monte Carlo simulations in Ref. [20], which is $T_c = 1.226\,03$. When there is no NNN interaction and the strength of the NN interactions $J_s > 2.041\,19$, the surface is in the extraordinary-log phase [20]. Starting with an extraordinary-log phase and tuning the surface NNN interactions J'_s of model (2), we get a phase diagram as shown in Fig. 1; the relevant critical behaviors will be shown in Sec. III.

For the simulations of the model, we adopt a combination of the local update (Metropolis algorithm) and the geometric cluster algorithm [27]. The geometric cluster algorithm improves the efficiency of the simulations, which is demonstrated in the Appendix. Each Monte Carlo step consists of five local updates and two geometric cluster updates. Each data point is an average over 10^7 Monte Carlo steps, and the largest system size we reached is $L = 128$. The surface variables we sampled include the surface squared (staggered) magnetization m_{s1}^2 and the surface magnetic susceptibility χ_{s1}, which are defined as

$$m_{s1}^2 = \langle\mathcal{M}_{s1}^2\rangle, \tag{4}$$

$$\chi_{s1} = L^2\left(\langle\mathcal{M}_{s1}^2\rangle - \langle|\mathcal{M}_{s1}|\rangle^2\right), \tag{5}$$

where $\mathcal{M}_{s1}$ is defined as

$$\mathcal{M}_{s1} = \frac{1}{L^2}\sum_{\vec{R}}(-1)^{x+y+z}\vec{\sigma}_{\vec{R}}. \tag{6}$$

Here, $\vec{R} = (x, y, z)$ is the coordination, where for the surface, z should be 1 or L, and L^2 is the number of sites of the surface. We also sample the sublattice squared (staggered) magnetization m_{s1A}^2, which is defined similar to (4), but the sites are restricted to be in sublattice A of the surface. Here, we have divided the square-lattice surface into two equivalent sublattices, because the square lattice is bipartite; sublattice A is one of two sublattices.

We also sample the surface specific heat C_{v1},

$$C_{v1} = L^2\left(\langle\mathcal{E}_1^2\rangle - \langle\mathcal{E}_1\rangle^2\right)/T^2, \tag{7}$$

where T is the temperature, and $\mathcal{E}_1$ is the microscopic energy density of the surface.

The surface correlation function is defined as

$$C_{\parallel}(r) = \langle\vec{\sigma}_i\cdot\vec{\sigma}_{i+r}\rangle, \tag{8}$$

where the site i and $i + r$ are restricted to be on the surface. The surface correlation length ξ_1 and "structure factor" F_1 are defined as

$$\xi_1 = \frac{\left(m_{s1}^2/F_1 - 1\right)^{1/2}}{2\sqrt{\sum_{i=1}^{d}\sin^2\left(\frac{k_i}{2}\right)}}, \tag{9}$$

$$F_1 = \frac{1}{L^4}\left\langle\left|\sum_{\vec{R}}(-1)^{x+y+z}e^{i\vec{k}\cdot\vec{R}}\vec{\sigma}_{\vec{R}}\right|^2\right\rangle, \tag{10}$$

where $\vec{k}$ is the "smallest wave vector" along the x direction, i.e., $\vec{k} \equiv (2\pi/L, 0)$. In the disordered phase, the correlation length ξ_1 is finite and the correlation ratio ξ_1/L decreases to zero, while in the ordered phase or extraordinary-log phase ξ_1/L diverges rapidly due to the rapid disappearance of the "structure factor" F_1. The correlation ratio ξ_1/L in the critical phase has a finite nonzero value in the thermodynamic limit. Therefore, the correlation ratio ξ_1/L is a good tool for locating the critical point of a phase transition.

III. RESULTS

A. Two special points

By using the Monte Carlo method, we simulate the antiferromagnetic Potts model (2) with an open boundary along the z direction and periodic boundaries along the x and y directions. At the bulk critical point [20] $T = T_c^{\text{bulk}} = 1.226\,03$, setting the system surface initially to the extraordinary-log phase ($J_s = 5$), and varying the surface NNN interactions J'_s, we can find two special points. As shown in Fig. 2(a), the surface magnetic susceptibility χ_{s1} of the system shows two peaks at $J_{sc}^{\prime(1)} \approx 0.85$ and $J_{sc}^{\prime(2)} \approx 3.3$, where the former peak diverges faster. The behaviors of the surface squared magnetization m_{s1}^2 and the surface structure factor F_1, as shown in Figs. 2(b) and 2(c), also demonstrate the two transitions. We can see that m_{s1}^2 tends to zero in the region between the two critical points, when the system is in an ordinary phase; we will discuss the properties of this phase specifically in the next section. The

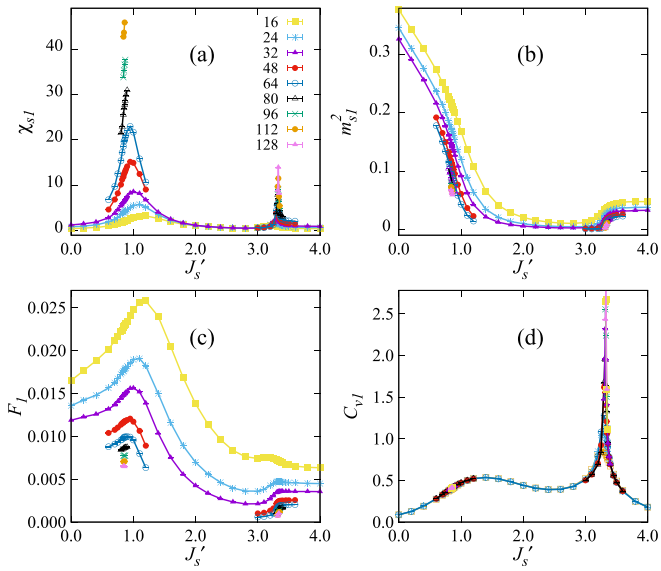

FIG. 2. Surface critical behaviors of the antiferromagnetic Potts model (2) at $T = T_c^{\rm bulk} = 1.226\,03$, $J_s = 5$: (a) Surface susceptibility χ_{s1}, (b) surface squared magnetization m_{s1}^2, (c) surface structure factor F_1, and (d) surface specific heat C_{v1}.

specific heat C_{v1}, as shown in Fig. 2(d), demonstrates a rapidly diverging peak at the second phase transition point; however, it does not show a diverging peak for the first phase transition.

In order to quantitatively determine the two critical points, we investigate the surface correlation ratio ξ_1/L, as shown in Fig. 3, which obviously shows the two critical points. In the vicinity of the critical point, ξ_1/L satisfies the finite-size

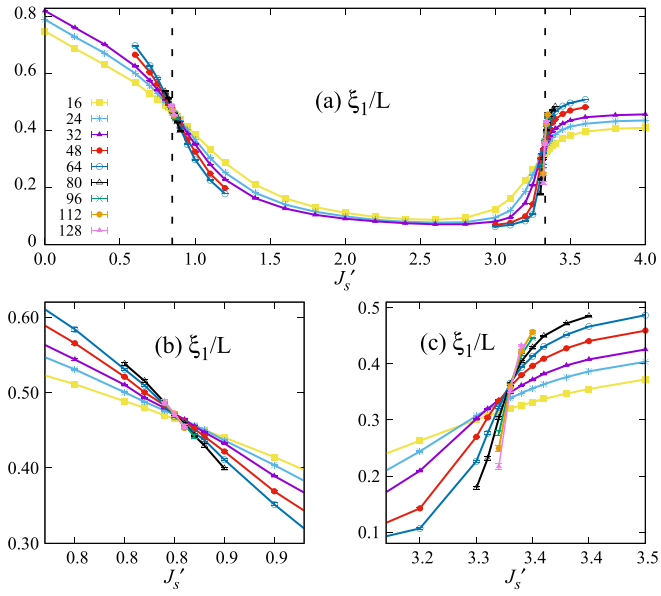

FIG. 3. Surface correlation ratio ξ_1/L of the antiferromagnetic Potts model (2) with $T = T_c^{\rm bulk} = 1.226\,03$ and $J_s = 5$; the dashed line positions in (a) are $J_{sc}'^{(1)} = 0.8478$ and $J_{sc}'^{(2)} = 3.3326$. (b) and (c) are the local enlargements of the vicinity of the two critical points, respectively.

TABLE I. Critical properties of the three-state antiferromagnetic Potts model (2), in correspondence to the phase diagram shown in Fig. 1. In all the data fitting, the correction-to-scaling exponent [30] y_1 is set to -0.789. SP = special point; Ord = ordinary phase; Ext-log = extraordinary-log phase; DOF = degree of freedom (in the data fitting); EQ = equation (used in the fitting).

Phase	Exponent	EQ	χ^2/DOF	$L_{\rm min}$	XY model
SP	$J_{sc}^{(1)} = 0.8478(9)$	(11)	1.42	32	
	$y_s = 0.59(3)$	(11)	1.42	32	0.608(4)[a]
	$y_{h1} = 1.698(4)$	(12)	0.89	48	1.675(1)[a]
	$\eta_\parallel = -0.399(5)$	(13)	1.84	16	
	$y_{h1A} = 0.26(3)$	(15)	0.48	16	
Ord	$y_{h1} = 0.77(2)$	(12)	0.55	32	0.781(2)[a]
Second SP	$J_{sc}^{(2)} = 3.3326(8)$	(11)	1.14	32	
	$y_s = 1.44(4)$	(11)	1.14	32	
	$y_{h1} = 1.56(2)$	(12)	1.19	24	
	$\eta_\parallel = -0.59(3)$	(13)	1.56	24	
	$y_{h1A} = 1.80(2)$	(15)	1.65	24	
Sublattice	$q = 0.57(3)$	(20)	1.32	32	0.59(2)[b]
Ext-log	$q = 0.59(3)$	(21)	1.43	32	
	$q_1 = 1.9(2)$	(22)	0.88	24	

[a]Reference [3].
[b]Reference [6].

scaling (FSS) formula

$$\xi_1/L = a_0 + \sum_{k=1}^{k_{\rm max}} a_k (J_s' - J_{sc}')^k L^{k y_s} + b L^{y_1}. \qquad (11)$$

This formula is derived from the theory of renormalization group (RG) [28,29], where $y_s > 0$ is the critical exponent, J_{sc}' is the critical point, and bL^{y_1} is the correction-to-scaling term, which comes from the irrelevant field of RG, with $y_1 < 0$; a_0, a_k, and b are nonuniversal parameters. For the first phase transition, the data of ξ_1/L are fitted according to (11) with $k_{\rm max} = 2$ and $y_1 = -0.789$ [30], which gives $J_{sc}'^{(1)} = 0.8478(9)$ and $y_s = 0.59(4)$ with $\chi^2/{\rm DOF} = 1.42$ (DOF = degree of freedom). It should be noted that the correction-to-scaling exponent $y_1 = -0.789$ comes from the study of the bulk criticality [30], and the reason why we take this value for the surface criticality is that all the surface criticalities are studied at the bulk critical point. The fitting results are listed in Table I. We can see that the critical exponent y_s coincides with the result of the well-known special transition of the XY model [3], which is $y_s = 0.608(4)$; in order to confirm that such a transition is in the same universality class of the XY model, we study the scaling behaviors of the squared magnetization m_{s1}^2 and the correlation function $C_\parallel(L/2)$, and at the critical point, they satisfy the following FSS formulas [28,29],

$$m_{s1}^2 L^2 = c + L^{2y_{h1}-2}(a + bL^{y_1}), \qquad (12)$$

$$C_\parallel(L/2) = L^{-1-\eta_\parallel}(a + bL^{y_1}), \qquad (13)$$

where y_{h1} and $\eta_\parallel$ are the critical exponents. The background term c in Eq. (12) comes from the contribution of the short-range correlation, in correspondence to the analytic part of the free energy. Such an analytic term does not appear in the

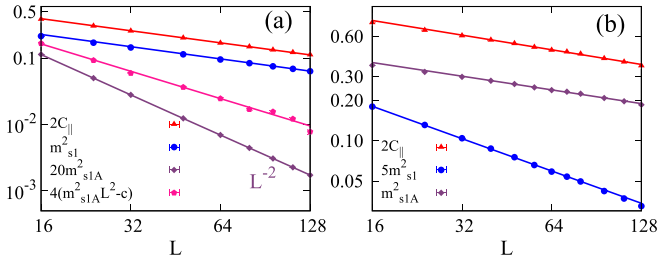

FIG. 4. (a) Log-log plot of $C_\parallel(L/2)$, m^2_{s1}, m^2_{s1A}, and $m^2_{s1A}L^2 - c$ vs L at the first transition point $J'^{(1)}_{sc} = 0.8478$. (b) Log-log plot of $C_\parallel(L/2)$, m^2_{s1}, and m^2_{s1A} at the second transition point $J'^{(2)}_{sc} = 3.3326$.

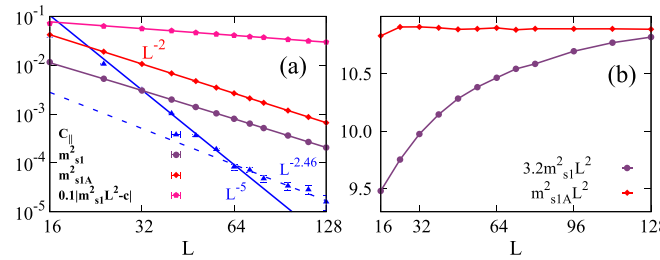

FIG. 5. (a) Log-log plot of the correlation function $C_\parallel(L/2)$, the squared magnetization m^2_{s1}, the sublattice squared magnetization m^2_{s1A}, and $|m^2_{s1}L^2 - c|$ for the ordinary phase, with $J'_s = 2.5$ and $c = 3.68$; (b) the data of $m^2_{s1}L^2$ and $m^2_{s1A}L^2$.

scaling formula of the correlation function $C_\parallel(L/2)$, because here we only consider the long-range correlation. The data fitting, with $y_1 = -0.789$, gives $y_{h1} = 1.698(4)$ and $\eta_\parallel = -0.399(5)$, where $\chi^2/\mathrm{DOF} = 0.89$ and 1.84, respectively. These results are also listed in Table I. We can see that the values of y_{h1} and $\eta_\parallel$ satisfy the scaling formula [31,32]

$$\eta_\parallel = d - 2y_{h1}, \tag{14}$$

where $d = 3$ is the space dimension of the system. This means that m^2_{s1} and $C_\parallel$ should decay with the same power as the increase of the system size, which is demonstrated in Fig. 4(a). We can also see that the value of y_{h1} coincides with that of the well-known special point of the XY model [3], which is $y_{h1} = 1.675(1)$, hence they belong to the same universality class.

We also investigate the scaling behaviors of the sublattice squared magnetization m^2_{s1A}, which is the same as m^2_{s1}; specifically, m^2_{s1A} satisfies

$$m^2_{s1A}L^2 = c + L^{2y_{h1A}-2}(a + bL^{y_1}), \tag{15}$$

where we have written the exponent as y_{h1A}. The data of m^2_{s1A} are also shown in Fig. 4(a). We can see that m^2_{s1A} shows a perfect power-law scaling, however, this is misleading, because such power-law scaling comes from the nonsingular part, which is the first term on the right-hand side of Eq. (15). Because in the current case $y_{h1A} < 1$, m^2_{s1A} is dominated by the term c/L^2. This is also the reason why we do not write the scaling form as $m^2_{s1A} = c/L^2 + L^{2y_{h1A}-4}(a + bL^{y_1})$. The log-log plot of $m^s_{s1A}L^2 - c$ vs L is also included in Fig. 4(a), and the data fitting according to Eq. (15) give $y_{h1A} = 0.26(3)$, with $\chi^2/\mathrm{DOF} = 0.48$. This result is also listed in Table I.

For the second special point, we fit the data according to Eq. (11) with $k_{max} = 3$ and $y_1 = -0.789$ [30], which gives $J'^{(2)}_{sc} = 3.3326(8)$ and $y_s = 1.44(4)$, with $\chi^2/\mathrm{DOF} = 1.14$. These results are also listed in Table I. We can see that the critical exponent y_s is obviously different from the first one; in order to determine the universality class of this transition, we investigate the scaling behaviors of the squared magnetization m^2_{s1} and the correlation function $C_\parallel(L/2)$; at the critical point, they satisfy the FSS formulas (12) and (13). By the data fitting, we get $y_{h1} = 1.56(2)$ and $\eta_\parallel = -0.59(3)$; these values are obviously different from the results of the first phase transition. Furthermore, we can see that they do not satisfy the scaling law (14), i.e., m^2_{s1} and $C_\parallel(L/2)$ decay with different powers, which are demonstrated in Fig. 4(b). In order to understand such a discrepancy and the nature of this phase transition, we investigate the sublattice squared (staggered) magnetization m^2_{s1A}, which is also shown in Fig. 4(b). The data fitting is performed similarly according to Eq. (15), which gives $y_{h1A} = 1.80(2)$. We can see that $\eta_\parallel$ and y_{h1A} satisfy the scaling law (14), i.e., $C_\parallel$ and m^2_{s1A} decay with the same power, as shown in Fig. 4(b). This result reveals the sublattice nature of such a transition. In summary, the second transition is characterized by the following critical exponents,

$$y_s = 1.44(4), \tag{16}$$

$$y_{h1} = 1.56(2), \tag{17}$$

$$y_{h1A} = 1.80(2), \tag{18}$$

$$\eta_\parallel = -0.59(3). \tag{19}$$

These results are also listed in Table I, including the fitting details.

B. The ordinary phase

For the intermediate region $J'^{(1)}_{sc} < J'_s < J'^{(2)}_{sc}$, the surface is in an ordinary phase. As shown in Fig. 5(a), the surface squared magnetization m^2_{s1} shows a very good power-law scaling, which is the effect of the nonsingular term c/L^2 because $y_{h1} < 1$ here. This situation is very similar to the case of the m^2_{s1A} at the first special point. In Fig. 5(a), we also show the log-log plot of $|m^2_{s1}L^2 - c|$ vs L, which also indicates a good power-law scaling; the data fitting according to Eq. (12) gives $y_{h1} = 0.77(2)$, with $\chi^2/\mathrm{DOF} = 0.55$. We find that the value of y_{h1} is consistent with that of the ordinary phase of the XY model [3], which is $y_{h1} = 0.781(2)$. These results are also listed in Table I.

For the sublattice squared magnetization m^2_{s1A}, the nonsingular part is also dominated by the L^{-2} scaling, as shown in Fig. 5(a), however, here we cannot perform an effective fitting of $m^2_{s1A}L^2$ according to the scaling formula (15), because $m^2_{s1A}L^2$ converges to the constant c too fast, as shown in Fig. 5(b); it can be compared to the data of $m^2_{s1}L^2$, which show very good asymptotic behavior, also shown in Fig. 5(b).

As to the scaling behavior of the surface correlation function $C_\parallel(L/2)$, we find that in the short-range region, it decays very fast, with a power of about L^{-5}; however, in the long-range region, it decays slower with a power of about $L^{2y_{h1}-4} = L^{-2.46}$. This is also illustrated in Fig. 5(a). It should be noted that the dashed line in Fig. 5(a) is not obtained by fitting

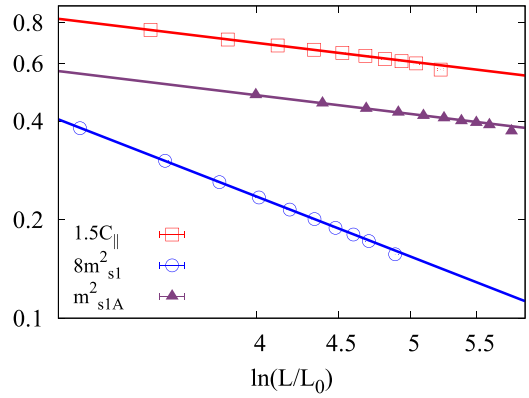

FIG. 6. Log-log plot of $C_{\parallel}(L/2)$, m_{s1}^2, and m_{s1A}^2 vs $\ln(L/L_0)$, with $J_s' = 3.8$ and $L_0 = 0.519$, 0.724, and 0.295 for the three variables, respectively. The slopes of the lines of $C_{\parallel}(L/2)$ and m_{s1A}^2 are $q = 0.59$, and the slope of m_{s1}^2 is $q_1 = 1.9$.

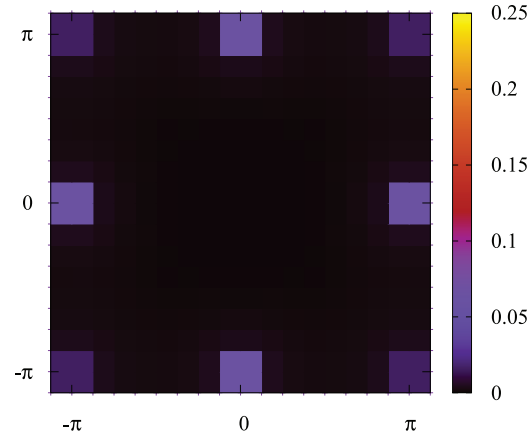

FIG. 7. Surface structure factor $F(\vec{k})$ for the extraordinary phase, with $J_s' = 3.8$; the system size is $L = 16$.

the long-range part data of $C_{\parallel}(L/2)$ but only a self-consistent check with $y_{h1} = 0.77$, which is obtained from the fitting of m_{s1}^2. The data in the long-range region are too small, which makes it too difficult to give accurate data in Monte Carlo simulations.

C. Sublattice extraordinary-log phase

We also try to investigate the properties of the phase with $J_s' > J_{sc}'^{(2)}$, but in this region, the efficiency of the algorithm decreases a lot, which makes it difficult to get good data for large systems. However, according to the already known results in our previous work [20] that strong enough surface NN interactions will lead to an extraordinary-log phase, we infer that the phase should be an extraordinary-log one; furthermore, because the NNN interactions are already very strong, we infer that the logarithmic decaying behaviors may be shown in the sublattices. To confirm such inference, we investigate the scaling behaviors of the surface correlation function $C_{\parallel}(L/2)$ and the sublattice squared magnetization m_{s1A}^2, and we find that they satisfy the logarithmic decaying formulas

$$C_{\parallel}(L/2) = a[\ln(L/L_0)]^{-q}, \tag{20}$$

$$m_{s1A}^2 = a[\ln(L/L_0)]^{-q}. \tag{21}$$

These formulas are subsequent finite-size scaling formulas of Eq. (1), which have been numerically verified in Refs. [5,6]. It is a different type of surface criticality, where the exponent q does not fall in the general scheme of a critical exponent, although it is also referred to as a "critical exponent" in some literature. The data fitting according to these formulas gives $q = 0.57(3)$ (from $C_{\parallel}$) and $q = 0.59(3)$ (from m_{s1A}^2). These results and also the details of the fitting are listed in Table I. We can see that the values of the decaying exponents for $C_{\parallel}(L/2)$ and m_{s1A}^2 coincide with each other, and they are also consistent with that of the XY model [6], which is $q = 0.59(2)$. These results are listed in Table I, including the fitting details; an illustrative plot of $C_{\parallel}(L/2)$ and m_{s1A}^2 is shown in Fig. 6.

We also investigate the squared magnetization m_{s1}^2, and we find that it also satisfies a logarithmic scaling formula

$$m_{s1}^2 = a[\ln(L/L_0)]^{-q_1}, \tag{22}$$

however, the decaying exponent is found to be $q_1 = 1.9(2)$, which is much different from q; this result and also the details of the fitting are listed in Table I, and the log-log plot of m_{s1}^2 vs $\ln(L/L_0)$ is also included in Fig. 6.

In order to further understand the properties of such a sublattice extraordinary-log phase, we compute the surface structure factor

$$F(\vec{k})) = \frac{1}{L^4}\left\langle \left| \sum_{\vec{R}} e^{i\vec{k}\cdot\vec{R}}\vec{\sigma}_{\vec{R}} \right|^2 \right\rangle \tag{23}$$

in the full momentum space (k_x, k_y). The result is shown in Fig. 7, in which we can see that the points $(0, \pm\pi)$ and $(\pm\pi, 0)$ are light, which means the system has a stripe order (in a finite system), which is in correspondence to the sublattice squared magnetization m_{s1A}^2. The points $(\pm\pi, \pm\pi)$ are also light but weaker than the points $(0, \pm\pi)$ and $(\pm\pi, 0)$, in correspondence to the squared magnetization m_{s1}^2.

We also investigate the symmetries of the two types of surface magnetization, as shown in Fig. 8, where we can see that both of them are O(2).

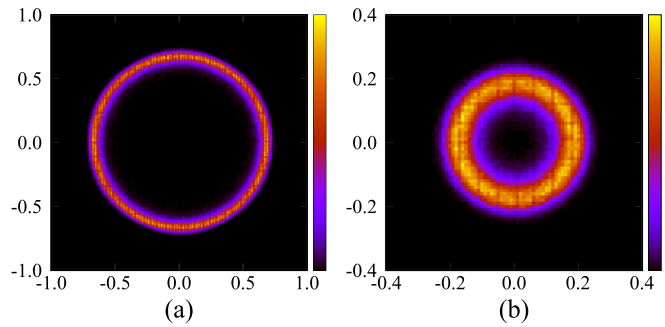

FIG. 8. Histograms of the two types of surface magnetization of the sublattice extraordinary-log phase, where $J_s' = 3.8$ and the system size $L = 32$. (a) Histogram of the sublattice magnetization of the surface. (b) Histogram of the (whole lattice) magnetization of the surface.

IV. CONCLUSION AND DISCUSSION

In summary, we have tried to add antiferromagnetic NNN interactions to the surface of the antiferromagnetic Potts model, with the extraordinary-log phase as the starting point. We find that as the NNN interactions increase, the system is driven to an ordinary phase in which the correlation function shares the same exponent of the ordinary phase of the XY model in the long-range region but decays much faster in the short-range region. Further strengthening the NNN interactions can drive the surface to an extraordinary-log phase whose main properties are shown in the sublattices of the surface. The special transition from the ordinary phase to the sublattice extraordinary-log phase belongs to a universality class that is different from the well-known special transition of the XY model.

It is well known that for a phase transition with spontaneous symmetry breaking, the universality class is determined by the dimension of space and the symmetry of the order parameter. For the special transition between the ordinary phase and the extraordinary-log phase, it is also the case, although the symmetry does not break in the extraordinary-log phase. Typical examples have been studied in the XY model [3], the Heisenberg model [5], the clock model [21], and the three-state antiferromagnetic Potts model [20]. For the antiferromagnetic Potts model we studied, the symmetries of the bulk critical point and the extraordinary-log phase are O(2) [20,24], which are the same as that of the XY model, and this is the reason why the special point (shown in Fig. 1) studied in the current paper belongs to the same universality of the special point of the XY model. For the second special point (also shown in Fig. 1), which is between the ordinary phase and the sublattice extraordinary-log phase, the reason why the universality class is different is also related to the symmetry; the symmetry in the sublattice extraordinary-log phase is $O(2) \times Z_2$, where the Z_2 symmetry originates from the equivalence of the two sublattices.

The present paper is closely related to Ref. [20], where in both papers we are following the idea that the surface criticality is a hybrid of the 3D bulk criticality and the 2D physics. In Ref. [20], the surface NNN interactions are ferromagnetic, while in the present paper the surface NNN interactions are antiferromagnetic; technically, the present paper is an extension of Ref. [20], however, the physical results are really very different. The reason is that a 2D (square lattice) three-state antiferromagnetic Potts model with ferromagnetic NNN interactions [25] is very different from that with antiferromagnetic NNN interactions [26]. Our results can be helpful in exploring the surface criticality.

ACKNOWLEDGMENTS

C.D. is supported by the National Science Foundation of China under Grant No. 11975024, and the Anhui Provincial Supporting Program for Excellent Young Talents in Colleges and Universities under Grant No. gxyqZD2019023. L.Z. is supported by the National Key R&D Program (2018YFA0305800), the National Natural Science Foundation of China under Grants No. 12174387 and No. 11804337, CAS Strategic Priority Research Program (XDB28000000), and CAS Youth Innovation Promotion Association. W.Z. was supported by the Hefei National Research Center for Physical Sciences at the Microscale (KF2021002).

APPENDIX: AUTOCORRELATION TIME OF THE ALGORITHMS

For a given variable f, the unnormalized autocorrelation function is defined as

$$C_f(t) = \langle f(0)f(t)\rangle - \langle f\rangle^2, \tag{A1}$$

where $f(t)$ means the microcosmic value of f at time t, and the unit of time is one Monte Carlo step. Then the normalized autocorrelation function is defined as

$$\rho_f(t) = C_f(t)/C_f(0). \tag{A2}$$

Based on $\rho_f(t)$, the integrated autocorrelation time is defined as [33]

$$\tau_{\text{int}} = \frac{1}{2}\sum_{t=0}^{\infty}\rho_f(t). \tag{A3}$$

In order to demonstrate the efficiency of the algorithms we adopt, we take f as the surface correlation $C_{\parallel}$ for example, and the results of τ_{int} for this variable are shown in Fig. 9. We can see that the autocorrelation of the combined algorithm composed of Metropolis and the geometric cluster is obviously smaller than that of the Metropolis algorithm only. Furthermore, τ_{int} is fitted according to

$$\tau_{\text{int}} = \tau_0 + bL^z, \tag{A4}$$

where z is the dynamical exponent that describes the efficiency of the algorithm, and τ_0 and b are nonuniversal parameters. For the combined algorithm, we get $z \approx 0.07$; for the Metropolis algorithm only, we get $z \approx 0.33$. This demonstrates that the geometric cluster algorithm improves the efficiency of the simulation.

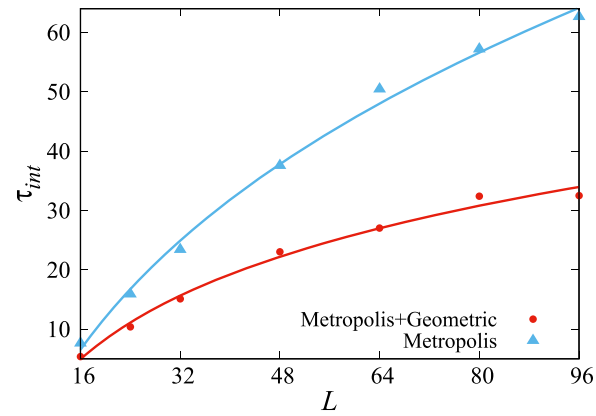

FIG. 9. Integrated autocorrelation time τ_{int} of the surface correlation function $C_{\parallel}$. The simulation is performed at the first special point shown in Fig. 3(b), where $T = T_c^{\text{bulk}} = 1.226\,03$, $J_s = 5$, and $J_s' = J_{sc}^{(1)} = 0.8478$.

[1] K. Binder, in *Phase Transitions and Critical Phenomena*, edited by C. Domb and J. L. Lebowitz, Vol. 8 (Academic Press, London, 1983).

[2] K. Binder and P. C. Hohenberg, Surface effects on magnetic phase transitions, Phys. Rev. B **9**, 2194 (1974).

[3] Y. Deng, H. W. J. Blöte, and M. P. Nightingale, Surface and bulk transitions in three-dimensional O(n) models, Phys. Rev. E **72**, 016128 (2005).

[4] Y. Deng, Bulk and surface phase transitions in the three-dimensional $O(4)$ spin model, Phys. Rev. E **73**, 056116 (2006).

[5] F. Parisen Toldin, Boundary Critical Behavior of the Three-Dimensional Heisenberg Universality Class, Phys. Rev. Lett. **126**, 135701 (2021).

[6] M. Hu, Y. Deng, and J.-P. Lv, Extraordinary-Log Surface Phase Transition in the Three-Dimensional XY Model, Phys. Rev. Lett. **127**, 120603 (2021).

[7] L. Zhang and F. Wang, Unconventional Surface Critical Behavior Induced by a Quantum Phase Transition from the Two-Dimensional Affleck-Kennedy-Lieb-Tasaki Phase to a Néel-Ordered Phase, Phys. Rev. Lett. **118**, 087201 (2017).

[8] C. Ding, L. Zhang, and W. Guo, Engineering Surface Critical Behavior of $(2+1)$-Dimensional O(3) Quantum Critical Points, Phys. Rev. Lett. **120**, 235701 (2018).

[9] L. Weber, F. Parisen Toldin, and S. Wessel, Nonordinary edge criticality of two-dimensional quantum critical magnets, Phys. Rev. B **98**, 140403(R) (2018).

[10] L. Weber and S. Wessel, Nonordinary criticality at the edges of planar spin-1 Heisenberg antiferromagnets, Phys. Rev. B **100**, 054437 (2019).

[11] M. A. Metlitski, Boundary criticality of the O(N) model in $d = 3$ critically revisited, SciPost Phys. **12**, 131 (2022).

[12] W. Zhu, C. Ding, L. Zhang, and W. Guo, Surface critical behavior of coupled Haldane chains, Phys. Rev. B **103**, 024412 (2021).

[13] L. Weber and S. Wessel, Spin versus bond correlations along dangling edges of quantum critical magnets, Phys. Rev. B **103**, L020406 (2021).

[14] C.-M. Jian, Y. Xu, X.-C. Wu, and C. Xu, Continuous Néel-VBS quantum phase transition in non-local one-dimensional systems with SO(3) symmetry, SciPost Phys. **10**, 033 (2021).

[15] F. Parisen Toldin and M. A. Metlitski, Boundary Criticality of the 3D O(N) Model: From Normal to Extraordinary, Phys. Rev. Lett. **128**, 215701 (2022).

[16] C. Ding, W. Zhu, W.-A. Guo, and L. Zhang, Special Transition and extraordinary phase on the surface of a two-dimensional quantum Heisenberg antiferromagnet, arXiv:2110.04762.

[17] X.-J. Yu, R.-Z. Huang, H.-H. Song, L. Xu, C. Ding, and L. Zhang, Conformal Boundary Conditions of Symmetry-Enriched Quantum Critical Spin Chains, Phys. Rev. Lett. **129**, 210601 (2022).

[18] W. Zhu, C. Ding, L. Zhang, and W. Guo, Exotic surface behaviors induced by geometrical settings of two-dimensional dimerized quantum XXZ model, arXiv:2111.12336.

[19] J. Padayasi, A. Krishnan, M. A. Metlitski, I. A. Gruzberg, and M. Meineri, The extraordinary boundary transition in the 3d O(N) model via conformal bootstrap, SciPost Phys. **12**, 190 (2022).

[20] L.-R. Zhang, C. Ding, Y. Deng, and L. Zhang, Surface criticality of antiferromagnetic Potts model, Phys. Rev. B **105**, 224415 (2022).

[21] X. Zou, S. Liu, and W. Guo, Surface critical properties of the three-dimensional clock model, Phys. Rev. B **106**, 064420 (2022).

[22] Y. Sun, J. Lyu, and J.-P. Lv, Classical-quantum correspondence of special and extraordinary-log criticality: Villain's bridge, Phys. Rev. B **106**, 174516 (2022).

[23] Y. Sun and J.-P. Lv, Quantum extraordinary-log universality of boundary critical behavior, Phys. Rev. B **106**, 224502 (2022).

[24] C. Ding, H. W. J. Böte, and Y. Deng, Emergent O(n) symmetry in a series of three-dimensional Potts models, Phys. Rev. B **94**, 104402 (2016).

[25] M. P. M. den Nijs, M. P. Nightingale, and M. Schick, Critical fan in the antiferromagnetic three-state Potts model, Phys. Rev. B **26**, 2490 (1982).

[26] Y.-H. Huang, L.-R. Zhang, and C. Ding, Critical behaviors of three-state antiferromagnetic Potts model on square lattice with next-nearestneighboring interactions (unpublished).

[27] J. R. Heringa and H. W. J. Blöte, Geometric cluster Monte Carlo simulation, Phys. Rev. E **57**, 4976 (1998).

[28] M. P. Nightingale, in *Finite-Size Scaling and Numerical Simulation of Statistical Systems*, edited by V. Privaman (World Scientific, Singapore, 1990).

[29] M. N. Barber, in *Phase Transitions and Critical Phenomena*, edited by C. Domb and J. L. Lebowitz, Vol. 8 (Academic Press, New York, 1983), see Ref. [1].

[30] R. Guida and J. Zinn-Justin, Critical exponents of the N-vector model, J. Phys. A **31**, 8103 (1998).

[31] M. N. Barber, Scaling relations for critical exponents of surface properties of magnets, Phys. Rev. B **8**, 407 (1973).

[32] T. C. Lubensky and M. H. Rubin, Critical phenomena in semi-infinite systems. I. ε expansion for positive extrapolation length, Phys. Rev. B **11**, 4533 (1975).

[33] A. D. Sokal, Monte Carlo methods in statistical mechanics: Foundations and new algorithms, in *Functional Integration*, edited by C. DeWitt-Morette, P. Cartier, and A. Folacci, NATO Advanced Studies Institute Vol. 361 (Springer, Boston, 1997), pp. 131–192.